THE ASTROPHYSICAL JOURNAL, 353:200–204, 1990 April 10

CCD IMAGERY OF PLANETARY NUCLEI: THE PROPERTIES OF THE CENTRAL STARS OF NGC 2440 AND NGC 7027

SARA R. HEAP[1] AND PAUL HINTZEN[1]
Laboratory for Astronomy and Solar Physics, Goddard Space Flight Center
Received 1988 September 9; accepted 1989 July 17

ABSTRACT

We report on the first results of a program of narrow-band imagery of planetary nebulae suspected of harboring exceedingly hot ($T > 300{,}000$ K), "massive" ($M \geq 1.0\ M_\odot$) central stars. Two of the most likely candidates are the nuclei of NGC 2440 and NGC 7027, for which Zanstra temperatures ~350,000 K have been reported, based on narrow-band continuum imaging data. However, even with carefully chosen passbands, the continuum nebular emission for such objects swamps the flux from the central star. We have therefore combined narrow-band CCD imaging (in Hβ, in He II 4686 Å, and in the line-free continuum) with image-subtraction techniques in order to isolate the central stars from the background nebulae, and to derive their magnitudes and Zanstra temperatures. We measure $V = 17.6 \pm 0.15$ for the nucleus of NGC 2440 and $V = 16.18 \pm 0.2$ for the nucleus of NGC 7027, leading to a value of $T_{\rm eff} \approx 200{,}000$ K for the central stars of both nebulae. Using published evolutionary tracks for planetary nuclei, we estimate central star masses of 0.62–0.70 $M_\odot$ for NGC 2440 and 0.65–0.70 for NGC 7027. These values are not much higher than the norm for planetary nuclei, which is estimated at 0.60 $M_\odot$.

Subject headings: nebulae: individual (NGC 2440, NGC 7027) — nebulae: planetary — spectrophotometry — stars: early-type

I. INTRODUCTION

Theoretical models predict that stars evolving up the asymptotic giant branch lose mass via a stellar wind, then slough off most of their remaining H-rich envelopes to become planetary nuclei (NPN) with masses ranging from 0.5 $M_\odot$ up to the Chandrasekhar limit, 1.4 $M_\odot$ (Paczyński 1971; Iben and Renzini 1983). Most observational evidence, however, indicates that nearly all central stars have nearly the same mass, ~0.60 $M_\odot$ (see Aller 1989; Mendez *et al.* 1988). The apparent dearth of high-mass ($M \geq 0.9$) central stars is not surprising in view of a near overwhelming selection effect: the time scale of evolution shortens drastically with increasing stellar mass. As an observational consequence, the time it takes for a nucleus to fade to 1/10th its early brightness (optical fading time) decreases with $M^{9.6}$ (Iben and Renzini 1983)! Despite selection effects, it would be reassuring to identify conclusively one or more "massive" central stars and thus, to have evidence for the broad range of masses predicted by evolutionary theory. We report here on an observing effort made to identify such stars.

Two likely high-mass candidates are the central stars of NGC 2440 and NGC 7027 (Tylenda 1984; Pottasch 1983, p. 218), but even these two are under debate. In both cases, the outcome of the debate hinges on the stellar magnitude, which does double duty in determining stellar temperature via the Zanstra method and bolometric luminosity. If the nucleus of NGC 2440 is as faint ($V = 18.9$) as Atherton *et al.* (1986) estimate, then the star is extremely hot ($T = 350{,}000$ K) and massive ($M = 1.0$) for a NPN, but (in their words) "the theory is incomplete" in that it cannot account for the long optical fading time. If on the other hand, the star is as bright ($V = 17.8$) as Heap (1987) estimated from *IUE* data, then the star is not so hot (merely 200,000 K!), it has a mass typical of planetary nuclei (0.6 $M_\odot$), and has other properties in accord with evolutionary theory. In the case of NGC 7027, the discrepancies in estimated stellar magnitude are even more severe. The central star of this nebula had not even been detected until 1979. In that year, Harlan and Miller (1979), using an image-tube camera and line-free filter detected the central star and estimated $V = 15 \pm 1$, while Atherton *et al.* (1979) derived $V = 19.4 \pm 1$ and $T_{\rm eff} = 350{,}000$ K from electronographic plates. Recently, two new estimates based on CCD imagery tend to bridge the gap ($V = 16.3$, Jacoby 1988; $V = 17.0$, Walton *et al.* 1988), but even these values are seriously discordant.

II. OBSERVING STRATEGY

According to evolutionary theory, the more massive the central star, the higher the maximum temperature it attains in its evolutionary course toward its final white-dwarf state. Typical planetary nuclei at 0.6 $M_\odot$ can get no hotter than ~140,000 K, and a 0.8 $M_\odot$ star no hotter than 250,000 K, whereas a 1.2 $M_\odot$ star reaches 650,000 K at its hottest point (Paczyński 1971). A direct way then to confirm the existence of massive central stars is to identify very hot stars ($T > 300{,}000$ K) embedded in young nebulae. Therein lies the observational challenge: a very hot star is *optically* fainter than a cooler star of the same bolometric luminosity; and young nebulae generally have high surface brightnesses that would mask the feeble optical emission from the central star. These two factors make it difficult to detect hot stars like those in NGC 2440 and NGC 7027, let alone measure stellar magnitude.

Given these difficulties, it is essential to observe these objects using CCD detectors with filter passbands free of nebular lines. But even this is not enough, because nebular *continuous* emission can still overpower the stellar emission. Our strategy for isolating a central star from its surrounding nebula is to use

[1] Visiting Astronomer, Kitt Peak National Observatory, a division of National Optical Astronomy Observatory, which is operated by the Associated Universities for Research in Astronomy, Inc., under contract with the National Science Foundation.

TABLE 1

DATA USED IN THE REDUCTION

Filter	λ_c (Å)	FWHM (Å)	k_λ (mag/airmass)	S_λ (10^{14} ergs/c)	$A_\lambda/E(B-V)$ (mag)	$m_\lambda - V$ (mag)
1	3930	28	0.384	1.474	4.46	−1.415
2	4690	38	0.215	4.787	3.84	−0.664
3	4765	9.5	0.204	5.000	3.77	−0.596
4	4865	40	0.190	5.386	3.681	−0.511

image-subtraction techniques: we subtract from a narrow-band continuum image a picture representing the continuous emission from the nebula. Nebular continuum emission scales as the Hβ flux, with the scale factor, K_λ, a slowly varying function of nebular temperature, density, and ionic helium abundance (Osterbrock 1974). We therefore obtain images in Hβ as well as in continuum passbands. The Hβ image scaled by K_λ then defines the surface of the nebular continuum emission, no matter how complicated that surface might be. We then subtract this scaled (and unreddened) Hβ image from the (unreddened) continuum image to obtain a picture of the central star alone.

Using J. P. Harrington's (private communication, 1983) computer program to calculate nebular continuous emission, we find the dominant sources to be hydrogen recombination and hydrogen two-photon emission, and recombination of doubly ionized helium. The latter is proportional to $N(He^{++})/N(H^+)$, so if the level of helium ionization varies within the nebula, then K_λ will also vary. The way we deal with this complication is to obtain images in the light of He II λ4686 as well as Hβ. From the ratio of these two absolutely calibrated and unreddened images, we determine the He^{++} abundance at each pixel (i, j)

$$\frac{N(He^{++})}{N(H^+)}_{ij} \approx R \, \frac{F_{ij}(\text{He II } \lambda 4686}{F_{ij}(\text{HB})} , \quad (1)$$

and then solve for the corresponding images of K_λ and the nebular background, $B_\lambda = K_\lambda F_\beta$. The constant of proportionality has a value, $R \approx 0.08$ for both NGC 2440 and NGC 7027.

Because the flux of a hot star rises toward shorter wavelengths faster than does the nebular flux, a maximum contrast of the star against the nebular background will be given by filters at wavelengths just longer than the Balmer limit at λ3646 (see Heap 1987, Fig. 1). Since we also need to exclude the Balmer series of hydrogen, we chose one filter passband to be centered at 3930 Å. Unfortunately, this passband is not completely free of nebular lines, such as He II λ3923, so we chose a second filter passband at 4765 Å, which should be completely clear of nebular lines. Table 1 gives information about the filters used in our observing program. Successive columns give filter number, central wavelength (λ_c), full-width at half-maximum transmission (FWHM), coefficient of atmospheric extinction (k) as determined in our observing run, effective sensitivity (S_λ), interstellar extinction coefficient at λ_c,

$$X_\lambda = A_\lambda / E_{B-V} , \quad (2)$$

and blackbody color of a very hot star

$$(m_\lambda - V)_0 = -2.5 \log F_\lambda(\lambda_c)/F_\lambda(V) \approx -2.5 \log (5480/\lambda_c)^4 . \quad (3)$$

TABLE 2

OBSERVATIONAL DATA AND RESULTS

ID	λ_c (Å)	n	Σt (s)	seeing FWHM(″)	$m_0(\lambda_c)$ (mag)	V (mag)
NGC 2440....	3930	6	4800	2.0	15.26	17.6
	4765	3	2200	2.2	15.8:	17.4:
NGC 7027....	3930	2	1600	1.8	...	...
	4765	1	800	1.8	12.70	16.2

III. OBSERVATIONS AND REDUCTION

The direct observations were obtained 1987 December 26–27 with a TI 800 × 800 CCD (with 2 × 2 on-chip summing) on the KPNO 2.1 m telescope. Because of a passing storm front, the seeing during the observing run was ~2″ FWHM. The mediocre seeing was unfortunate: according to Atherton *et al.* (1986), in 1″ seeing the central star of NGC 2440 was readily detected, while in 2″ seeing it could not be identified at all. In fact, we were able to detect (barely) the central star in our raw continuum data even at 2″ seeing.

During the run, we acquired 120 useful pictures of 12 planetaries and a photometric standard star, G191−B2B. Table 2 gives a summary catalog of observations for NGC 2440 and NGC 7027. Successive columns list filter and central wavelength, number of observations in the co-added image, total exposure time, seeing (FWHM), measured unreddened magnitude at the filter wavelength, and the derived apparent V magnitude. Integration times were limited to 15 minutes to prevent contamination of the region of interest by charge from bad columns at one edge of the CCD chip. Because of this limitation, we often used the wider λ3930 filter as the primary continuum passband, despite modest contamination from lines, rather than the line-free λ4765 filter.

As part of the reduction procedure, we applied to each image (1) a correction for atmospheric extinction, (2) an absolute calibration, and (3) a correction for interstellar extinction, with $E(B-V) = 0.30$ for NGC 2440 (Gathier, Pottasch, and Pel 1986), and $E(B-V) = 0.93$ for NGC 7027 Pottasch 1984). We used a set of 18 images of G191−B2B for determining extinction coefficients and for absolute calibration. We have observed this star over a range of zenith distances which included the zenith distances of the program stars. There is no indication that the extinction coefficients changed over the observing run. The extinction coefficients (Table 1) are close to the standard coefficients for Kitt Peak.

On a separate observing run, P. H. obtained a spectrophotometric scan of GR191−B2B, which we used to determine the absolute calibration for each filter. As a check on the calibration, we observed NGC 2392, which has a relatively bright and cool central star embedded in a low surface brightness nebula. The resulting V magnitude for this star ($V = 10.53$) is reasonably close to previous photoelectric measurements (see Acker 1982). As another check, we compared our measured Hβ nebular fluxes of seven nebulae with previous results and found no differences greater than $\Delta \log F_\beta = \pm 0.06$.

Because of the limitation on exposure time, it was necessary to co-add short exposures in the continuum filters (Number 1 and 3). To do this, we first used the software package. DAOPHOT (Stetson 1987), to measure on each image the positions of all field stars, which we used as geometric fiducials for registration. After shifting each picture to achieve the proper registration (one-tenth of a pixel), we then co-added the series of pictures.

IV. NGC 2440

Figure 1 (Plate 1) shows six pictures of NGC 2440: at the top (*a* and *b*), an Hβ image at two different contrast levels; the co-added image in Filter 1 (λ3930) in (*c*); a representation of $E(B-V)$ in (*d*); the residual, stellar image in (*e*); and in (*f*) the ionization ratio, $N(\mathrm{He}^{++})/N(\mathrm{H}^+)$ from equation 1. Figure 2 shows cross sectional profiles of NGC 2440 taken through the central star as obtained with the continuum filter 1 (λ3930). In either figure, the central star is barely visible above the nebular background in the narrow-band continuum filter, but it is clearly visible in the residual picture. The nebular emission is strongly saddle shaped, a circumstance that would doom any attempt to interpolate for the background under the stellar image. The dashed curves of Figure 2 outline the estimated nebular profile as determined by the Hβ scaling method outlined in § II and described in detail in the next paragraph.

The level of ionization given by $F_{ij}(\lambda 4686)/F_{ij}(\mathrm{H}\beta)$ (eq. [1]) varies significantly across the nebula. The ionization ratio reaches a maximum of 0.09 ~ 2″ SW of the central star (not at the central star). The scaling factor for this high-ionization region is estimated at $K_\lambda = 1.59 \times 10^{-3}$ Å^{-1}, considerably higher than the nebular average, $K_\lambda = 1.31 \times 10^{-3}$ (based on $T_e = 14{,}000$, $N_e = 3000$, $N(\mathrm{H}^+) = 0.06$, $N(\mathrm{He}^{++}) = 0.053$, as determined by Shields *et al.* 1981). Allowing for a variable K_λ across the nebula, we then calculated the nebular continuum-background image

$$B_{ij} = K_{ij} F_{ij}(\mathrm{HB}) + L F_{ij}(\mathrm{He\ II}\ \lambda 4686)\ , \quad (4)$$

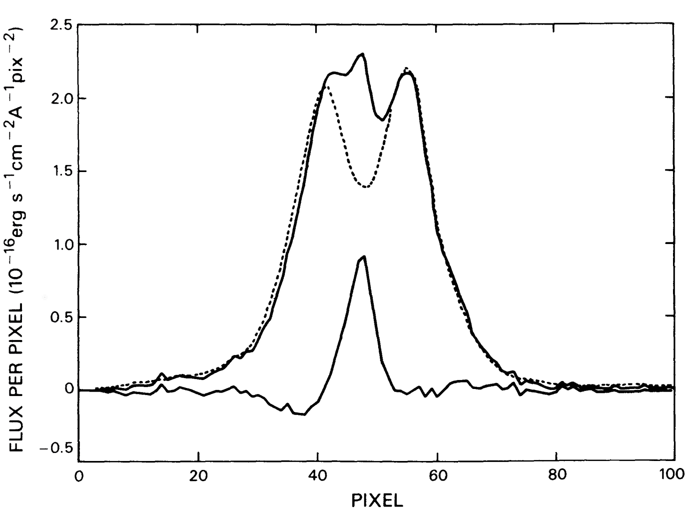

FIG. 2.—Cross sectional profiles across NGC 2440. The abscissa gives pixel number (0″.38 per pixel) and the ordinate, unreddened flux per pixel. The upper solid line gives the observed flux profile in the light of the 3930 Å continuum filter, while the dashed line shows the estimated nebular flux profile at this filter wavelength. The lower solid curve shows the residual, stellar profile.

where the rightmost term accounts for contributions from He II λ3923 transmitted by filter 1. Spectroscopic measurements (Kaler 1976) give a value for the unreddened intensity ratio, $L = I(\lambda 3923)/I(\lambda 4686) = 0.01$, while theoretical estimates suggest $L = 0.008$ (Osterbrock 1974). We consider the value of L as a parameter to be determined by comparison with observation and obtain $L = 2 \times 10^{-4}$ with an upper limit $L = 4 \times 10^{-4}$.

The residual stellar image (Fig. 1*e*) is round with a FWHM = 2″.0, the same as other stars in the field. The sum of the positive flux elements in the stellar image with a circular aperture of 12 pixels (4″.6) leads to an unreddened stellar magnitude at the continuum filter wavelength, $m_0(\lambda 3930) = 15.26 \pm 0.15$, where stellar magnitude is defined as

$$m_\lambda = -2.5 \log F_\lambda - 21.115\ . \quad (5)$$

Accounting for stellar light lost outside the 12 pixel aperture yields a correction of -0.10 mag; however, allowing for residual nebular light within the aperture gives a $+0.10$ mag correction. Since these two corrections cancel each other, we adopt m (λ3930) = 15.26. We now convert to apparent visual magnitude using the formula

$$V = m_0(\lambda) - (m_\lambda - V)_0 + 3.1\ E_{B-V}\ , \quad (6)$$

to obtain $V = 17.6 \pm 0.15$ for $E(B-V) = 0.30$. This value of V is considerably brighter than the estimate ($V = 18.9$) of Atherton *et al.* (1986), but it is in keeping with Heap's (1987) results ($V = 17.8$) from *IUE* data. We believe that this new $V = 17.6$ is more reliable than either previous determination. Furthermore, it is in accord with a recent measurement, $V = 17.7 \pm 0.13$, by Jacoby (private communication, 1988), who used a nebular-subtraction technique similar to ours. Given a distance of 2190 pc as derived by Gathier, Pottasch, and Pel (1986), we obtain an absolute magnitude for the central star, $M_v = +14.96$.

Our procedure for deriving the apparent V magnitude—which involves dereddening with an adopted $E(B-V)$, image subtraction, and subsequent reddening with the same $E(B-V)$—should not be affected by the value of $E(B-V)$ used. (We adopted $E(B-V) = 0.30$ from Gathier, Pottasch, and Pel 1986). However, we do find evidence for variable extinction across the face of the nebulae, with $E(B-V)$ rising from southeast to northwest. The evidence comes from a comparison of the observed ratio of continuous fluxes at λ3930 and λ4765 to the theoretical ratio (Fig. 1*d*). That is, away from the central star, the color excess at pixel (i, j) is given by

$$m(\lambda 3930) - m(\lambda 4765) = -2.5 \log K_{3930}/K_{4765} + (X_{3930} - X_{4765}) E_{B-V}\ . \quad (7)$$

For NGC 2440, $E(B-V) = \Delta m/0.70$, except at the position of the central star, where this formula is invalid. (Thus, the apparent hole in the extinction at the location of the central star [Fig. 1*d*] is not necessarily correct.) In practice, equation (7) is difficult to apply, because the λ3930 filter transmits He II λ3923 line emission as well as continuum emission. However, after correcting for the contribution of the line emission, we obtain $E(B-V) = 0.1$ in the SE lobe of the nebula increasing to $E(B-V) = 0.3$ in the NW lobe. For the nebula as a whole, we obtain $E(B-V) = 0.21$, midway between $E(B-V) = 0.30$ obtained from radio and Hβ fluxes, and $E(B-V) = 0.12$ derived from the Balmer decrement (Gutierez-Moreno, Moreno, and Corres 1985).

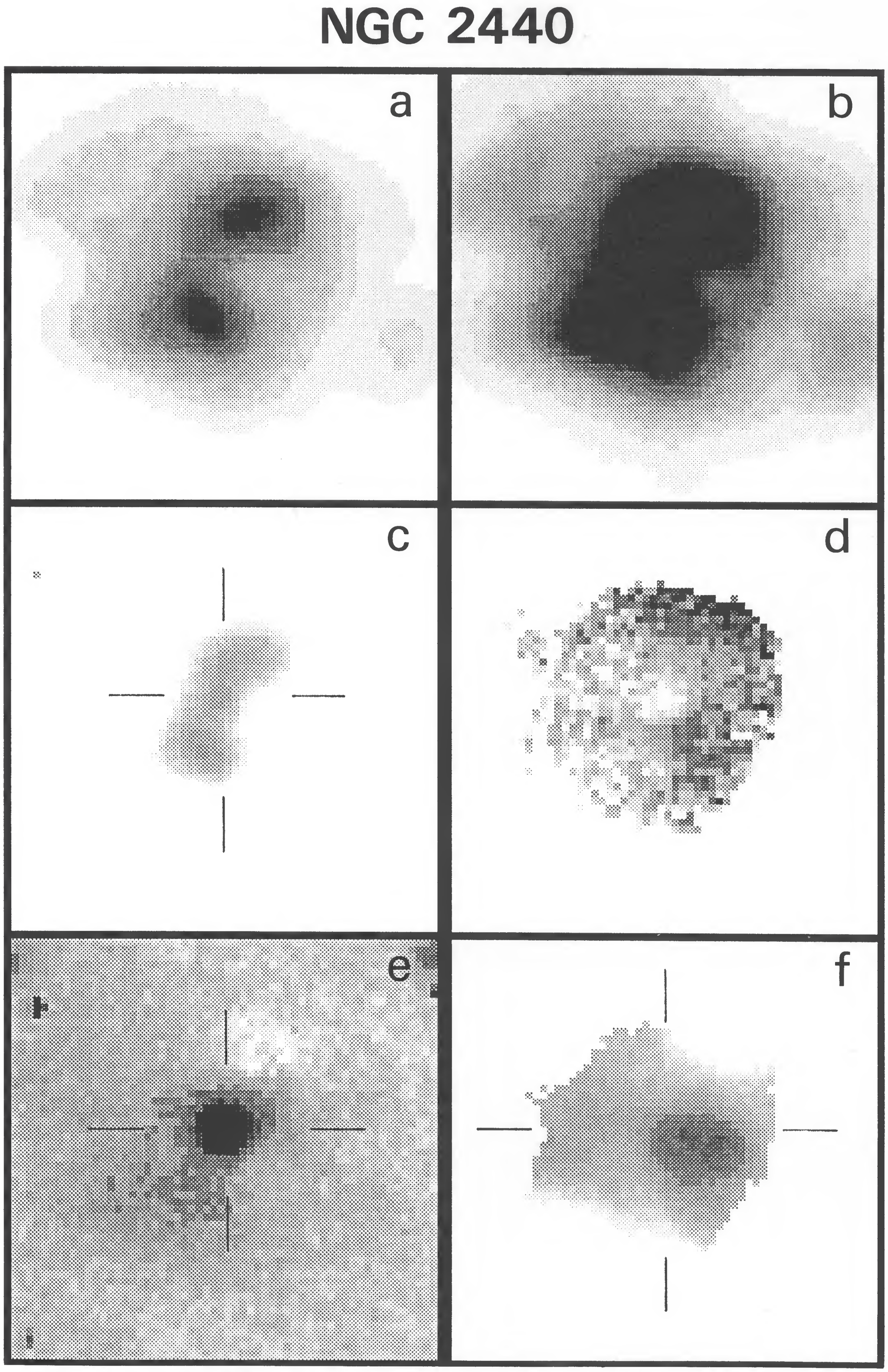

FIG. 1.—Images of NGC 2440. (*a*) and (*b*) show Hβ images at two different contrast levels, (*c*) shows the co-added λ3930 continuum image, (*d*) shows $E(B-V)$, (*e*) is the residual continuum image, and (*f*) represents the ionization ratio, $N(He^{++})/N(H^{+})$.

HEAP AND HINTZEN (*see* **353**, 202)

In computing the Zanstra temperature for the central star, we used Pottasch's (1984) formulae applied to stellar and nebular fluxes corrected for reddening, viz.

$$[F(\mathrm{H}\beta)_0/F_\lambda(V)_0] = 3.95 \times 10^{-11} T^3 G_1(T) \times (e^{2.665E4/T} - 1) , \quad (8a)$$

$$[F(4686)_0/F_\lambda(V)_0] = 8.49 \times 10^{-11} T^3 G_4(T) \times (e^{2.665E4/T} - 1) . \quad (8b)$$

where the functions G_1 and G_4 are tabulated by Pottasch. For $V = 17.6$, our measured nebular fluxes, log $F(\mathrm{H}\beta) = -10.57$, log $F(4686) = -10.76$, and a uniform $E(B-V) = 0.30$, we obtain the two Zanstra temperatures, T_z(H I) = 199,000 K and T_z(He II) = 192,000 K, results that are virtually indistinguishable from Heap's (1987) estimate of temperature.

Given an adopted temperature, $T = 200{,}000$ K, we derive a stellar radius, $R = 0.038\ R_\odot$, and a bolometric luminosity, $L = 2100\ L_\odot$. Comparison of the star's position on an H-R diagram with evolutionary tracks for planetary nuclei (Wood and Faulkner 1983), as shown in Figure 3*a*, indicates that the central star is a 0.70 $M_\odot$ star, which has finished its horizontal track across the H-R diagram and is now a hot white dwarf.

The kinematic age of the nebula, as derived from the nebular expansion velocity and present size, can be used as the timekeeper of stellar evolution. The position of the nucleus of NGC 2440, defined by $M_v = +5.0$, $t = 7100$ yr (Heap 1987), on Schoenberner's (1981) optical-fading diagram for planetary nuclei, as reproduced in Figure 3*b*, suggests a somewhat smaller stellar mass, $M = 0.62\ M_\odot$, than is inferred from its position on an H-R diagram. It also predicts a stellar temperature of 165,000 K, somewhat lower than observed, but it is in accord with Aller's (1989) estimate of stellar temperature (180,000 K) based on nebular models. Neither of these discrepancies is considered serious.

V. NGC 7027

Figure 4 (Plate 2) shows the same six pictures of NGC 7027 as were shown by Figure 1 for NGC 2440, except that the narrow-band continuum picture (Fig. 4*c*) and residual image (Fig. 4*e*) are for filter 3 (λ4765). Figure 5 shows cross-sectional profiles of NGC 7027 at λ4765. As with NGC 2440, the star is only marginally visible in the narrow-band continuum image, but it is the dominant star in the residual image. In contrast to NGC 2440, the ionization level of NGC 7027 is low, mainly because its high-density enforces rapid recombination. The ionization structure of the inner region (Fig. 4*f*) appears as a shallow basin, with the star midway between the center, where $N(\mathrm{He}^{++})/N(\mathrm{H}^+) = 0.03$, and the more highly ionized rim where $N(\mathrm{He}^{++})/N(\mathrm{H}^+) = 0.04$. Since filter 3 is free of nebular lines, the nebular background is calculated as

$$B_{ij} = K_{ij} F_{ij}(\mathrm{H}\beta) , \quad (9)$$

where the scaling factor is computed to be $K_\lambda = 0.776 \times 10^{-3}$ at the location of the central star.

Again, using an aperture 12 pixels in diameter and accounting for the flux lost outside the aperture ($0^{\mathrm{m}}09$), we obtain $m_0(4765) = 12.70 \pm 0.2$, or $V = 16.18 \pm 0.2$. While in wild disagreement with the $V = 19.4$ magnitude given by Atherton *et al.* (1979), our estimate is in accord with a recent measurement, $V = 16.32 \pm 0.35$, by Jacoby (1988), who used an image-subtraction technique similar to ours. Both our and Jacoby's values of V are substantially brighter than $V = 17.0$ derived by Walton *et al.* (1988), who attempted to measure the stellar flux directly from a narrow-band continuum image.

Atherton *et al.* (1979) found strong evidence for variable reddening across the face of the nebula. More recently, Walton

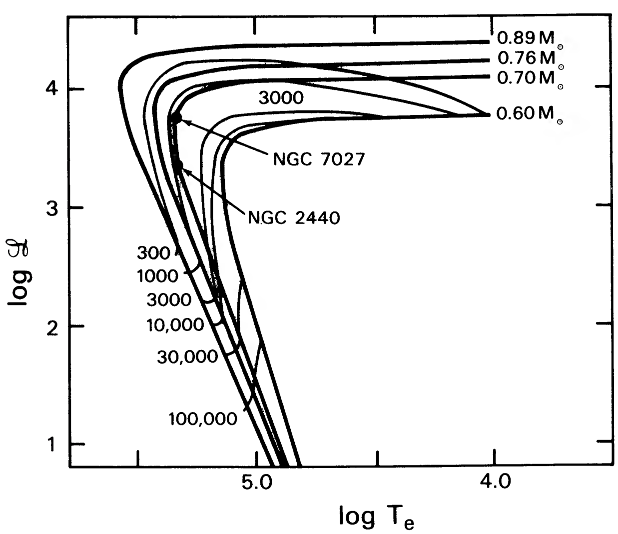

FIG. 3*a*

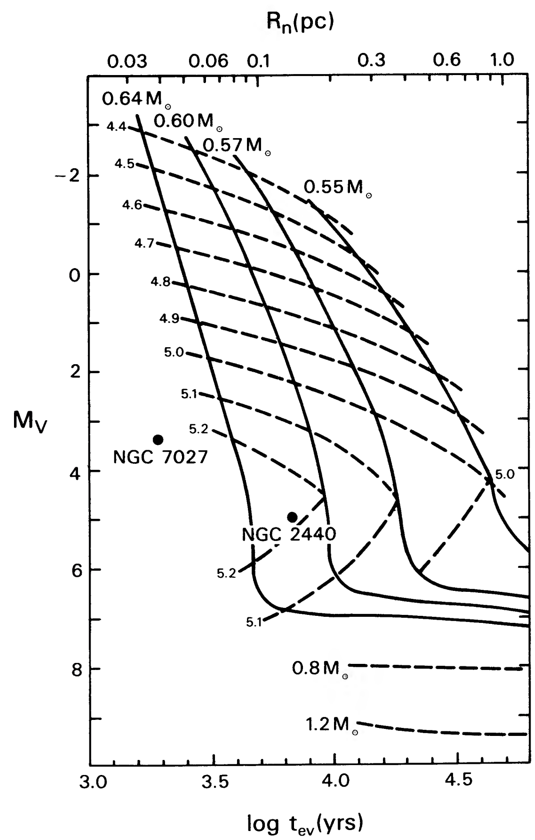

FIG. 3*b*

FIG. 3.—Comparison of the observed properties with predictions. Fig. 3*a* shows a comparison with evolutionary tracks on an H-R diagram computed by Wood and Faulkner (1983). The heavy lines are tracks for planetary nuclei of the specified mass. The thin lines define contours of equal evolutionary time, in yr, since log $T_{\mathrm{eff}} = 4.0$. Fig. 3*b* shows a comparison with evolutionary tracks on the optical-fading diagram (Schoenberner 1981) and labeled with the central-star mass. Lines of constant effective temperature are represented by dashes and labeled with values of log T_{eff}.

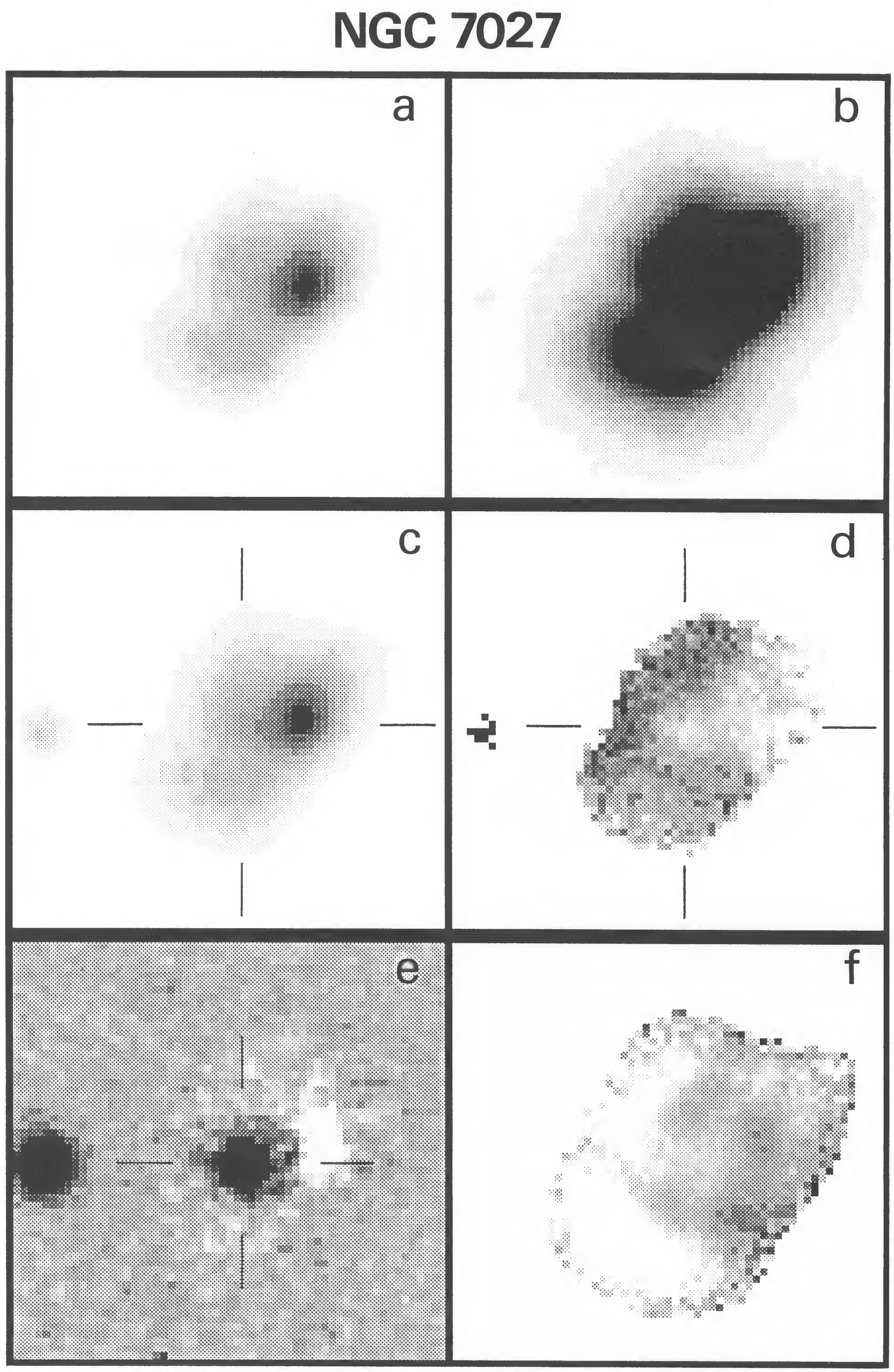

FIG. 4.—Images of NGC 7027. (*a*) and (*b*) show Hβ images at two different contrast levels, (*c*) shows the λ4745 continuum image, (*d*) shows $E(B-V)$ across the nebula, (*e*) is the residual continuum image, and (*f*) represents the ionization ratio, $N(\mathrm{He}^{++})/N(\mathrm{H}^{+})$.

HEAP AND HINTZEN (*see* **353**, 203)

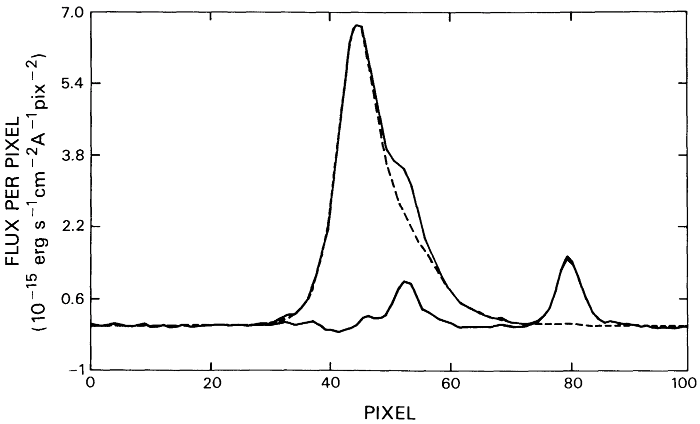

FIG. 5.—Cross sectional profiles across NGC 7027 for the 4765 Å filter, similar to those for NGC 2440 in Fig. 2.

et al. (1988) derived a map of $E(B-V)$ from radio and Hβ images of the nebula. They found that at the position of the central star, $E(B-V) = 0.8$, while on the average, the nebula has a color excess, $E(B-V) = 1.0$. We have evidence for variable reddening which conforms to the map by Walton *et al.* (Fig. 3*d*), although we are not able to say anything about the color excess at the position of the star. Using equation (7) with $F(\lambda3930)$ corrected for nebular line contributions, we obtain an average $E(B-V) = 0.95$ for the whole nebula.

In computing the Zanstra temperature of the central star, we follow Walton *et al.* (1988) by correcting the stellar flux with $E(B-V) = 0.8$ to obtain $V_0 = 13.68$ while correcting the nebular flux with $E(B-V) = 0.93$. Again, using Pottasch's (1984) formulae and tables, we obtain T_z(H I) = 226,000 K, and T_z(He II) = 194,000 for the nucleus of NGC 7027. The fact that the hydrogen Zanstra temperature is higher than the He II Zanstra temperature is not surprising in light of Stasinska and Tylenda's (1986) demonstration that for temperatures higher than ~200,000 K, T_z(H I) tends to overestimate the true stellar temperature because each He^{++} photon produces more than one hydrogen-ionizing photon. We therefore adopt $T = 200,000$ K for the central star of NGC 7027.

The distance to NGC 7027 is quite uncertain, with estimates ranging from 178 pc (Daub 1982) to 1500 pc (Pottasch *et al.* 1982). Here, we adopt Masson's (1986) distance of 940 ± 200 pc derived from radio expansion measurements to obtain an absolute stellar magnitude, $M_v = +3.4$. With this distance combined with the measured stellar temperature and (unreddened) visual flux, we derive a radius, $R = 0.065\,R_\odot$, and luminosity, $L = 6000\,L_\odot$, for the central star. These properties suggest that the nucleus is a 0.70 $M_\odot$ star that has just finished traversing the high-luminosity, horizontal track in the H-R diagram.

The size of the nebula, and therefore the kinematic age, is also uncertain. Pottasch (1984) lists the angular radius of NGC 7027 at $\theta = 4''$, while Walton *et al.* (1988) found that nebular emission extends out to $\theta = 23''$. If the source of this faint emission is, in fact, the planetary nebula (as opposed to the remnant red-giant wind), then the kinematic age could be as high as 5000 yr. We estimate the angular radius of the nebula at 8″. The position of the star ($M_v = +3.4$, $t = 1800$ yr) on the optical-fading diagram indicates that the star has a mass somewhat greater than 0.64 $M_\odot$.

VI. CONCLUSIONS

From narrow-band CCD imagery, we derive the following properties for the central star of NGC 2240: $V = 17.6$, $M_v = 5.0$, $T = 200,000$ K, $R = 0.038$, $L = 2100$, and $M = 0.62$ (from evolutionary diagram) or $M = 0.70$ (from H-R diagram). For the central star of NGC 7027, we obtain $V = 16.2$, $M_v = +3.4$, $T = 200,000$ K, $R = 0.064$, $L = 6000$, and $M > 0.64$ (evolutionary diagram) or $M = 0.70$ (H-R diagram). Neither star lives up to its billing as a "high-mass" central star. Instead, both appear to be ≈0.70 $M_\odot$ stars, with the nucleus of NGC 2440 being the slightly more highly evolved of the two.

Note added in Manuscript—In 1988 July, we obtained narrow-band images at Hα, Hβ, λ4800, and He II λ4686 of NGC 7027 at the CFH telescope in sub-arcsec seeing. The central star is prominent in the narrow-band continuum picture at 4800 Å. The data indicate that $E(B-V) = 0.88$ near the star and $E(B-V) = 1.02$ further out in the nebula; $m_0(4800) = 12.64$ or, $V = 16.14$. Thus, the CFHT observations confirm the results presented in this paper.

We thank the KPNO staff for assistance with observing and initial data reductions. We also thank the referee, George Jacoby, for suggestions which improved the presentation of the paper. P. H. was supported by NASA RTOP 188-41-51-07.

REFERENCES

Acker, A., *et al.* 1982, *Catalogue of the Central Stars*, (Pub. C.D.S.), No. 3.
Aller, L. H. 1989, in *IAU Symposium 131*, *Planetary Nebulae*, ed. S. Torres-Peimbert (Boston: Kluwer), p. 306.
Atherton, P. D., *et al.* 1979, *Ap. J.*, **232**, 786.
Atherton, P. D., *et al.* 1986, *Nature*, **320**, 423.
Daub, C. T. 1982, *Ap. J.*, **260**, 512.
Gathier, R., Pottasch, S. R., and Pel, J. W. 1986, *Astr. Ap.*, **151**, 171.
Gutierrez-Moreno, A., Moreno, M., and Cortes, G. 1985, *Pub. A.S.P.*, **97**, 397.
Harlan, E. A., and Miller, J. S. 1979, *Pub. A.S.P.*, **91**, 168.
Heap, S. R. 1987, *Nature*, **326**, 571.
Heap, S. R., and Augensen, H. 1987, *Ap. J.*, **313**, 268.
Iben, I., and Renzini, A. 1983, *Ann. Rev. Astr. Ap.*, **21**, 271.
Jacoby, G. 1988, *Ap. J.*, **333**, 193.
Kaler, J. B. 1976, *Ap. J. Suppl.*, **31**, 517.
Masson, C. R. 1986, *Ap. J.* (*Letters*), **302**, L27.
Mendez, R. H., Kudritzki, R. P., Herrero, A., Husfeld, D., and Groth, H. G. 1988, *Astr. Ap.*, **190**, 113.
Osterbrock, D. 1974, *Astrophysics of Gaseous Nebulae* (San Francisco: Freeman).
Paczyński, B. 1971, *Acta Astr.*, **21**, 417.
Pottasch, S. R. 1981, *Astr. Ap.*, **94**, L13.
———. 1984, *Planetary Nebulae* (Dordrecht: Reidel).
Pottasch, S., Goss, W., Arnal, E. M., and Gathier, R. 1982, *Astr. Ap.*, **106**, 229.
Schoenberner, D. 1981, *Astr. Ap.*, **103**, 119.
Shields, G. A., Aller, L. H., Keyes, C. D., and Czyzak, S. J. 1981, *Ap. J.*, **248**, 569.
Stasinska, G., and Tylenda, R. 1986, *Astr. Ap.*, **155**, 137.
Stetson, P. 1987, *Pub. A.S.P.*, **99**, 191.
Tylenda, R. 1984, *Astr. Ap.*, **138**, 317.
Walton, N., Pottasch, S. R., Reay, N. K., and Taylor, A. R. 1988, *Astr. Ap.*, **200**, L21.
Wood, P. R., and Faulkner, D. J. 1983, *Ap. J.*, **307**, 659.

SARA R. HEAP and PAUL HINTZEN: Code 681, Goddard Space Flight Center, Greenbelt, MD 20771